

# 3D-Image Reconstruction in Highly Collimated 3D Tomography

Robert Azencott, *University of Houston and ENSC France*, Bernhard G. Bodmann, *University of Houston*, Demetrio Labate, *University of Houston*, Anando Sen, *University of Houston*, Igor Patrikeev, *University of Texas Medical Branch*, Massoud Motamedi, *University of Texas Medical Branch*

**Abstract**—The paper introduces a novel method for image reconstruction in 3D tomography, called Searchlight Computed Tomography, which reduces the overall radiation exposure when primarily the reconstruction of a specified region of interest is required. To achieve this goal, the Searchlight CT approach restricts the acquisition essentially to X-rays passing through the region of interest of a 3D object, yet the algorithm provides a stable and robust reconstruction of the region of interest. The Searchlight CT algorithm is based on an iterative procedure for which generic conditions for the convergence are provided. Its performance is validated on experimental data.

**Index Terms**—X-ray Transform, Radon Transform, 3D Computed Tomography, Inverse Problems

## I. INTRODUCTION

Computed Tomography (CT) is a widely used medical imaging method which is employed to visualize interior organs within the human body and obtain information of their structural properties. Starting with its introduction in the 1970s, CT has become an essential tool in medical diagnostic and preventive medicine, and its usage has increased very rapidly over the last decade due to technological advances which have made the procedure much more user-friendly to both patients and radiologists<sup>1</sup>. In particular, in recent years, the application of CT has been expanded rapidly due to the introduction of new imaging technology such as 64-detector scanners for applications such as angiography [8], [13]. However, the acceptance of new imaging instruments has been slow in past due to concerns about radiation safety and the dose that is needed [12], [9] to acquire CT images with high spatial resolution. Furthermore, in preclinical studies where high-resolution CT technique could be routinely used for longitudinal imaging of animal models, there is a great need for reducing radiation dose during imaging studies of tumors. Nevertheless, by its nature, CT involves the exposure of the patient to X-ray radiation and this is associated with health risks (in the form of radiation-induced carcinogenesis) which are essentially proportional to the levels of radiation exposure. Indeed, it is estimated that currently about 2% of cancers in the United States may be attributed to the radiation from CT examinations [4].

The method presented in this paper aims to reduce the overall radiation exposure from CT when primarily the reconstruction of a specific region of interest within the human body or within an organ is required. This is the typical situation,

for example, of patients undergoing regular CT screenings to monitor the progress of a tumor (when longitudinal studies with frequent scanning are needed). It is clear that, if the objective is to reconstruct only a “small” region of interest within a 3D object, it is possible in principle to dramatically reduce the radiation dose during a CT scan by using *collimated* X-ray projections, i.e., by limiting the irradiation mainly to the X-ray passing through the region of interest. Indeed, in this paper we show that it is possible to reconstruct a specific region of interest in collimated three-dimensional X-ray tomography by employing a new reconstruction algorithm which ensures numerically stable and accurate reconstruction. The new algorithm, called Searchlight Computed Tomography, is based on an iterative procedure, which converges rapidly inside the region of interest and whose performance was validated on both synthetic and experimental data. The development of this new algorithm, which is able to maintain image quality while reducing incident dose of radiation, could have significant impact on the field of biomedical imaging.

Before proceeding with the description of the algorithm, let us recall the basic definitions which are used in X-ray Tomography.

### A. X-ray Transform and its Inversion

The objective of X-ray Tomography consists in converting a set of projection images of a three-dimensional object, usually obtained by measuring the attenuation of a certain radiation travelling along various directed paths, into a representation of the object structure [5]. The X-ray transform is the mathematical model used to establish a formal relationship between the observed data (i.e., the projection images) and the object under investigation. Specifically, for a compactly supported Lebesgue-integrable function  $F$  on  $\mathbb{R}^3$ , its **X-ray transform**  $XF$  is a function defined on the set of all straight lines  $l$  in  $\mathbb{R}^3$ . That is, for  $w \in \mathbb{R}^3$  and  $\theta$  a unit vector in  $\mathbb{R}^3$ , the X-ray Transform of  $F$  at  $(w, \theta)$  is the line integral of  $F$  over the straight line  $l(w, \theta)$ , through  $w$  with direction  $\theta$ , defined by

$$XF(w, \theta) = \int_{-\infty}^{\infty} F(w + t\theta) dt. \quad (1)$$

The objective of recovering  $F$  from the values of  $XF$  is formally achieved by inverting the X-ray transform. Unfortunately, this is a classical ill-posed problem, in the sense the reconstructing  $F$  from the values of its X-ray transform is numerically unstable. This numerical instability becomes even

<sup>1</sup>Over 72 million CT scans were performed in the USA in 2007 [19].

more challenging if one desires to recover  $F$ , or part of it, from an incomplete set of X-ray data [15].

The classical formula for the inversion of the X-ray transform is the so-called Filtered Back-projection which is an application of the classical Fourier Slice Theorem [1], [14]. Namely, for an integrable function  $F$  on  $\mathbb{R}^3$ , we have

$$\begin{aligned} F(x, y, z) &= X^{-1}(XF)(x, y, z) \\ &= \int_{\mathbb{R}^3} \mathcal{F}_2(X_{\theta(\xi)}F)(\xi) e^{i((x,y,z)\cdot\xi)} d\xi, \end{aligned} \quad (2)$$

where  $X_{\theta}F(w) = XF(w, \theta)$ ,  $\mathcal{F}_2$  denotes the 2D Fourier transform on a plane  $h(\theta(\xi))$  with normal vector  $\theta(\xi)$ , and  $\theta(\xi)$  is any vector orthogonal to  $\xi$ .

### B. Collimated X-ray Transform

In this paper, we are interested in a special instance of reconstruction from incomplete data where the goal is the reconstruction of a specific region of interest  $S$  of an unknown 3D object  $F$  using mainly the X-rays passing through  $S$ . As expected, direct reconstruction attempts from collimated X-ray projections introduce many undesirable artifacts due to the ill-posedness of the inversion problem, so that some form of regularized reconstruction is required. The regularized reconstruction method which is introduced in this paper is based on an iterative procedure which is able to provide accurate reconstructions of a specific region of interest  $S$  mainly employing the collection of X-rays collimated on  $S$ .

Let us start by defining the precise mathematical model for the collimated X-ray tomography. Since we are interested in reconstructing  $F$  inside a spherical region  $S \subset I^3$ , when mainly the X-rays passing through  $S$  are used in the acquisition, in view of of this, we denote the fully retained part of the X-ray transform as,

$$T = \{(w, \theta) : l(w, \theta) \cap S \neq \emptyset\}$$

and let  $U = T^C$ . Hence, to model the modified acquisition, we define the **collimated X-ray transform** by

$$\tilde{X}F(w, \theta) = e^{-d(w, \theta)^2 R/r^2} XF(w, \theta), \quad (3)$$

where  $d(w, \theta)$  denotes the distance of the line  $l(w, \theta)$  from  $S$ ,  $r$  is the radius of  $S$  and  $R$  is a parameter describing the attenuation of the rays not passing through the region of interest (in our numerical tests,  $R = 460$  was used). Note that, when  $(w, \theta) \in T$ , then  $\tilde{X}F(w, \theta) = XF(w, \theta)$ .

Our objective is to obtain an accurate approximation of the unknown function  $F$  in the region of interest  $S$  from  $\tilde{X}F$ .

## II. SEARCHLIGHT CT COLLIMATED RECONSTRUCTION

A major step in our iterative reconstruction algorithm is the repeated regularization of the estimated values of  $F$  outside the region of interest  $S$ . To this end, we partition the complement of  $S$  into subsets  $\{Q_j\}$ , each one of fixed volume  $\text{vol}(Q_j) = v$ , and perform local averages. Hence, the regularization operator  $\sigma$  is given by:

$$\sigma F(x, y, z) = \begin{cases} F(x, y, z) & (x, y, z) \in S, \\ \tau(F, Q_j) & (x, y, z) \in Q_j, \end{cases} \quad (4)$$

where  $\tau(F, Q_j) = \frac{1}{v} \iiint_{Q_j} F(x, y, z) dx dy dz$ . Clearly, several variants of the regularization operator  $\sigma$  can be employed, but will not be considered here for brevity.

The **Searchlight CT algorithm** is initialized by setting  $G = \tilde{X}F = 1_T \cdot XF$ , where  $F$  is the unknown density function and the dot denotes point-wise multiplication, and by computing the initial approximation of  $F$  as  $f_0 = X^{-1}G$ . The subsequent approximations  $f_n$ ,  $n \geq 1$ , of  $F$  are obtained through the following iterative procedure.

- 1) Compute  $\sigma f_n$  as in (4).
- 2) Compute  $X\sigma f_n$ , the standard X-ray Transform of  $\sigma f_n$ , using (1). By projecting the data into the complementary sets  $T$  and  $U$ , write

$$X\sigma f_n = 1_T \cdot X\sigma f_n + 1_U \cdot X\sigma f_n$$

- 3) Replace  $1_T \cdot X\sigma f_n$  by the known data  $G = 1_T \cdot XF$  in the preceding formula to define  $Y_n = G + 1_U \cdot X\sigma f_n$ .
- 4) Compute  $f_{n+1}$  by applying the X-ray Inversion formula (2) to  $Y_n$ . Hence,

$$f_{n+1} = X^{-1}Y_n = X^{-1}[G + 1_U \cdot X\sigma f_n]. \quad (5)$$

Under mild assumptions, the sequence of functions  $f_n$  converges to the unknown density function  $F$  inside the region of interest  $S$  [2].

## III. NUMERICAL DEMONSTRATIONS

The Searchlight CT algorithm for collimated reconstruction was validated first on a set of 3D Shepp-Logan Phantoms (tests not reported here) and then on two sets of 3D biological data, namely data from a human jaw and a mouse. Representative 2D slices extracted from the reconstructed three-dimensional region of interest are reported in Figures 1 and 2, and compared against the standard filtered back-projection reconstructions.

In our tests, collimated acquisition was simulated assuming that the X-ray emitting source is located at arbitrary (discrete) positions on a fixed sphere outside the unknown object  $F$ . Each data set  $F$  (phantoms or biological data) considered has size of  $257^3$  voxels. The regions of interest  $S$  were chosen to be spherical regions with a radius larger than 40 voxels and center which is not the center of the sphere of source positions, in general. The complement of  $S$  in  $I^3$  was partitioned in 8-voxels cubes. The size of the (simulated) planar 2D set of acquisition sensors was kept fixed and equal to  $452 \times 370$  voxels for all source positions. The distance between the center of this planar set of sensors and the source position was also kept constant.

### A. Performance of the Collimated Reconstruction

The performance of the Searchlight CT algorithm in terms of the accuracy of the reconstruction inside the region of interest was evaluated by various performance measures, which are described below.

For any voxel  $u = (x, y, z)$ , let  $F(u)$  and  $F_{rec}(u)$  be the original and reconstructed functions, respectively. The

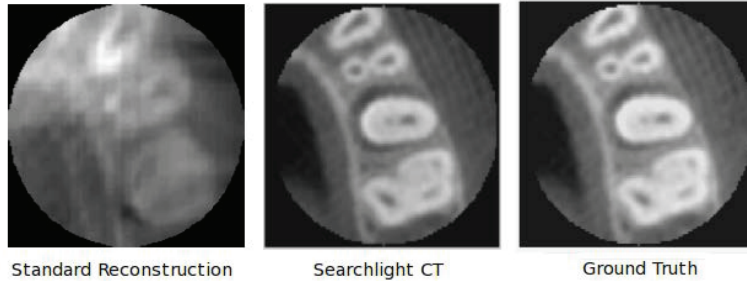


Fig. 1. Reconstruction comparison for an axial CT view of region from human jaw (data from Dr.Bhagia).

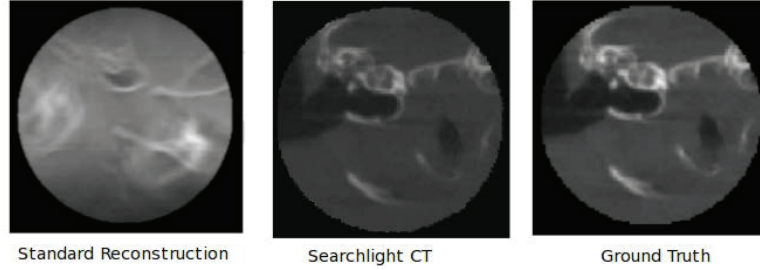


Fig. 2. Reconstruction comparison for an axial micro-CT view of mouse abdominal region (data from Center of Biomedical Engineering, UTMB).

**Relative Reconstruction Error**,  $Rel$  is defined as,

$$Rel = \frac{\sum_{v \in S} |F(u) - F_{rec}(u)|}{\sum_{u \in S} F(u)} \quad (6)$$

As expected, the application of the direct standard filtered back-projection method produces unacceptable inaccuracies and artifacts when applied to collimated data. In fact, for collimated data generated from a typical Shepp-Logan phantom, standard uncollimated reconstruction operators yields a Relative Reconstruction Error  $Rel = 23.6\%$  whereas the proposed Searchlight CT algorithm yields  $Rel = 9.5\%$ . The Searchlight CT result is obtained after 40 iterations, which is approximately the number of iterations required for the algorithm to converge. Similar performance is achieved using the biological data. Specifically, in the case of the human jaw data (see Figure1) Searchlight CT (40 iterations) yields  $Rel = 9.9\%$  vs.  $Rel = 28.1\%$  in the case of standard reconstruction; in the case of the adult mouse data (see Figure 2) the values are  $Rel = 10.3\%$  (40 iterations) vs.  $Rel = 26.7\%$ .

#### B. Criteria for Performance of Reconstruction

The radiation dose  $d(u)$  received by a voxel  $u$  is defined as the number of rays passing through  $u$ . Let  $c = \sum_{u \in I^3} d(u)$  be the sum of received doses over all voxels, in the case of collimated irradiation, and  $m$  be the maximal dose which is received in the uncollimated case. We define the **Radiation Exposure**  $EX$ , as

$$EX = \frac{c}{m}. \quad (7)$$

When  $EX$  increases, the reconstruction improves and hence  $Rel$  reduces. This is illustrated in Figure 3, using the mouse data set.

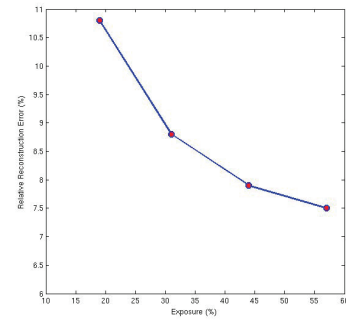


Fig. 3. Relative Reconstruction Error vs Radiation Exposure plot

TABLE I  
PERFORMANCE VS. RADIUS OF REGION OF INTEREST

Radius of $S$	$D$	$EX$	$Rel$	PSNR
45 voxels	4.0 %	19 %	10.8 %	53.1 dB
60 voxels	9.9 %	31 %	8.8 %	58.2 dB
75 voxels	20.7 %	44 %	7.9 %	60.7 dB
90 voxels	29.8 %	57 %	7.5 %	61.9 dB

As discussed in [2], the spherical region of interest  $S$  must be sufficiently large to ensure the convergence of Searchlight CT algorithm. Specifically, the size of  $S$  should be chosen to satisfy certain conditions on the notion of **Relative Density**  $D$  of a region  $S$ , which is defined as the ratio between the sum of densities over the voxels inside  $S$  and the sum of densities over all voxels. Our numerical tests show that  $D$  must be higher than 2.5% to ensure accurate collimated reconstruction. Table I summarizes the performance of the Searchlight CT algorithm (using the mouse data), measured in terms of  $EX$ ,  $Rel$ ,  $D$  and PSNR, as the radius of the regions of interest varies between 45 and 90 voxels. If the radius is below 40 voxels,  $D$  falls

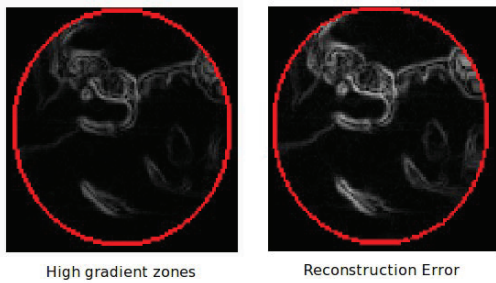


Fig. 4. The comparison of the two plots shows that there is high correlation between the edges location of and the points with large reconstruction error.

below 2.5% and the reconstruction fails.

### C. Comparison with the literature

The problem of reconstruction from incomplete X-ray data has received significant attention in the literature. However, most of the work currently available is focused on the 2D case, such as in [16], [18]. For the sake of comparison, we have developed a 2D version of our algorithm and compared it against the method proposed in [16], using a 2D Shepp-logan phantom as a data set. It turns out that our collimated reconstruction algorithm yields  $Rel = 4.1\%$ , vs.  $Rel = 7.7\%$  obtained using the method from [16] and  $Rel = 11.2\%$  obtained from standard filtered back-projection. Another major difference is the exposure  $EX$ , which is 27% for our algorithm, vs. 45% for the algorithm in [16].

Other methods proposed in the literature focus on only extracting the singular part (i.e., edges) of the data [10], [11], [17], [3], [7], [6], and are not comparable with our approach.

### D. Detailed Analysis of Error

The Relative Reconstruction Error provides a global measure of the error. A closer look at the algorithm performance shows that the reconstruction error is mostly localized in correspondence of the points where the function  $F$  is discontinuous, i.e., along the edges. This behaviour is illustrated in Figure 4, where, for a representative 2D slice of  $F$  inside the region  $S$ , we have displayed side by side the gradient of  $F$  and the locations where the reconstruction error is large. The correlation between edge locations and large-error points is confirmed by the the histograms for the distribution of errors over the region  $S$  and on the zone of high gradient (calculated using the 85th quantile), which is shown in Figure 5.

## IV. CONCLUSION

The Searchlight CT algorithm provides a promising approach for preserving accurate image reconstruction in 3D tomography while significantly reducing the incident dose of radiation. Practical implementations of the algorithms could be beneficial in clinical and preclinical applications for improving margins of imaging safety by selective image targeting.

### ACKNOWLEDGMENT

This work was partially supported by NSF DMS 0604561 and a two year Methodist Hospital grant.

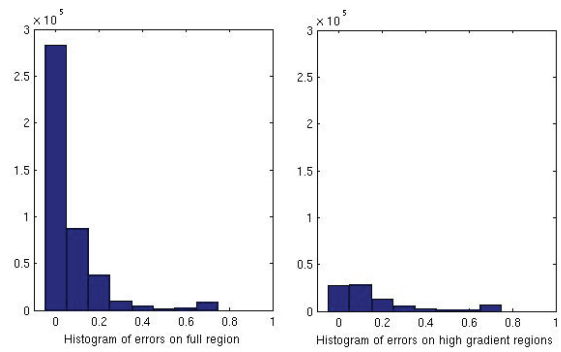


Fig. 5. Comparison between the histograms of Relative Errors in the whole region of interest  $S$  and in the subregions of high gradient

## REFERENCES

- [1] A. Averbuch and Y. Shkolnisky. 3D discrete x-ray Transform. *Applied and Computational Harmonic Analysis*, 17:259–276, 2004.
- [2] R. Azencott, B. Bodmann, D. Labate, A. Sen, K. Li, and X. Zhou. Searchlight CT: A new reconstruction method for collimated x-ray tomography. *Proceedings NCMIP*, 2011.
- [3] C. Berenstein and D. Walnut. Local inversion of the radon transform in even dimensions using wavelets. In *In 75 Years of Radon Transform*, S. Gindikin and P. Michor, editors., pages 45–69. International Press, 1992.
- [4] D. Brenner and E. J. Hall. Computed tomography. an increasing source of radiation exposure. *N Engl J Med.*, 357:2277–2284, 1997.
- [5] C. Epstein. *Introduction to the Mathematics of Medical Imaging, Second Edition*. SIAM: Society for Industrial and Applied Mathematics, 2007.
- [6] A. Faridani, D. Finch, E. Ritman, and K. Smith. Local tomography II. *SIAM Journal of Applied Mathematics*, 57(4):1095–1127, 1997.
- [7] A. Faridani, E. Ritman, and K. Smith. Local tomography. *SIAM Journal of Applied Mathematics*, 51:459–484, 1193–1198, 1992.
- [8] C. Herzog, P. L. Zwerner, and J. R. Doll et al. Significant coronary artery stenosis: comparison on per-patient and per-vessel or per-segment basis at 64-section ct angiography. *Radiology*, 244(1):112–120, 2007.
- [9] W. Huda, W. Randazzo, and S. Tipnis et al. Embryo dose estimates in body ct. *AJR Am J Roentgenol*, 194(4):874–880, 2010.
- [10] A. Katsevich. Improved cone beam local tomography. *Inverse Problems*, 22:627–643, 2006.
- [11] A. Katsevich and A. Ramm. Pseudolocal tomography. *SIAM Journal of Applied Mathematics*, 56(1):167–191, 1996.
- [12] C. I. Lee, A. H. Haims, and E. P. Monico et al. Diagnostic ct scans: assessment of patient, physician, and radiologist awareness of radiation dose and possible risks. *Radiology*, 231(2):393–398, 2004.
- [13] J. M. Miller, M. Dewey, and A. L. Vavere et al. Coronary ct angiography using 64 detector rows: methods and design of the multi-centre trial core-64. *Eur Radiol*, 19(4):816–828, 2009.
- [14] F. Natterer. *The Mathematics of Computerized Tomography*. SIAM: Society for Industrial and Applied Mathematics, 2001.
- [15] F. Natterer and F. Wubbeling. *Mathematical Methods in Image Reconstruction*. SIAM: Society for Industrial and Applied Mathematics, 2001.
- [16] T. Olson and J. Destefano. Wavelet localization of the radon transform. Technical Report PCS-TR93-196, Dartmouth College, Computer Science, Hanover, NH, 1993.
- [17] E. Quinto. Singularities of the X-ray transform and limited data tomography in  $R^2$ . *SIAM Journal of Mathematical Analysis*, 24:1215–1225, 1993.
- [18] F. Rashid Farrokhi, K. Ray Liu, C. Berenstein, and D. Walnut. Wavelet-based multiresolution local tomography. *IEEE Transactions on Image Processing*, 6(10):1412–1429, 1997.
- [19] R. Smith-Bindman, J. Lipson, R. Marcus, M. M. K. Kim, R. Gould, A. B. de Gonzalez, and D. Miglioretti. Radiation dose associated with common computed tomography examinations and the associated lifetime attributable risk of cancer. *Arch Intern Med.*, 169(22):2078–2086, 2009.
- [20] J. Yang, H. Yu, M. Jiang, and G. Wang. High-order total variation minimization for interior tomography. *Inverse Problems*, 26:1–29, 2010.